Medical Engineering & Physics 35 (2013) 269–276

Contents lists available at SciVerse ScienceDirect

Medical Engineering & Physics

journal homepage: www.elsevier.com/locate/medengphy

Inertia sensor-based guidance system for upperlimb posture correction

Z.Q. Ding[a], Z.Q. Luo[a], A. Causo[a,*], I.M. Chen[a], K.X. Yue[a], S.H. Yeo[a], K.V. Ling[b]

[a] School of Mechanical and Aerospace Engineering, Nanyang Technological University, Singapore
[b] School of Electrical and Electronic Engineering, Nanyang Technological University, Singapore

ARTICLE INFO

Article history:
Received 2 February 2011
Received in revised form 31 August 2011
Accepted 4 September 2011

Keywords:
Posture correction
Posture measurement
Posture replication
Vibrotactile feedback
Inertia sensor
IMU

ABSTRACT

Stroke rehabilitation is labor-intensive and time-consuming. To assist patients and therapists alike, we propose a wearable system that measures orientation and corrects arm posture using vibrotactile actuators. The system evaluates user posture with respect to a reference and gives feedback in the form of vibration patterns. Users correct their arm posture, one DOF at a time, by following a protocol starting from the shoulder up to the forearm. Five users evaluated the proposed system by replicating ten different postures. Experimental results demonstrated system robustness and showed that some postures were easier to mimic depending on their naturalness.

1. Introduction

Demand on the healthcare system rises in proportion to the aging population. Technology can fill in the supply gap by providing automated systems to augment healthcare services [1]. For rehabilitation, the advent of small inertia-based sensors and feedback devices like vibrotactile actuators could help improve healthcare delivery.

Micromachined accelerometers, gyroscopes, and magnetometers are sufficiently small to be attached to the human body without interfering with movement. Accelerometers are used as inclinometer for motion where acceleration with respect to gravity are negligible while gyroscopes measure angular velocity and provide estimate in orientation change. Magnetometers determine the local earth magnetic field vector and provide additional information about orientation. These sensors are packaged together to form an inertial measurement unit (IMU), which is relatively cheap and consumes little energy.

IMU had been employed in posture measurement and rehabilitation: quantifying hemiparesis by measuring hand path in pointing tasks [2], treating idiopathic scoliosis [3], and detecting and assessing severity of Parkinson's disease [4]. Moreover, accelerometers had been used to detect trunk posture [5], and inertia sensors to measure full body motion [6] and determine gait kinematics [7]. Other technologies that have been proven effective in stroke patient rehabilitation include functional electrical stimulation (FES) for artificial activation of the skeletal muscles [8,9].

Interestingly, sensing user movement may not be sufficient. Feedback from therapists also plays an important role in informing patients of their progress leading to better chances of recovery [10]. Feedback can be audio, visual, tactile, or any combination thereof. Audio feedback was used in [11], where patients adjusted their trunk posture depending on feedback quality. In [12], audio and visual cues from the teacher were aided by a robotic suit that employed tactile feedback to guide the movement of the upper limb. Vibrotactile was used in [13] to improve dynamic gait of the elderly. Improvements in motion performance of Tai-Chi practitioners were realized using vibrotactile feedback complemented with audio feedback [14]. In [15,16], visual and tactile feedback were used to guide the subjects in replicating the target arm posture. A comparison of selected works is presented in Table 1.

The works cited demonstrate the robustness of inertia-based sensors in measuring limb, trunk, or full body posture and the importance of feedback in correctly replicating the desired postures. This paper presents a system that uses inertia-based sensors to measure arm posture and vibrotactile actuators to guide arm posture correction. Also presented is a protocol in measuring complete arm posture that requires only two IMUs and two vibrotactile actuators.

The optimized design combination of inertia sensors and vibrotactile feedback to correct arm posture is the main contribution of this paper. The system finds the balance between number of inertia sensors needed and the number of joints (DOFs) that has

* Corresponding author. Tel.: +65 90873849.
E-mail addresses: zqding@ntu.edu.sg (Z.Q. Ding), zqluo@ntu.edu.sg (Z.Q. Luo), acauso@gmail.com (A. Causo), chen@ntu.edu.sg (I.M. Chen), yue@ntu.edu.sg (K.X. Yue), yeosh@ntu.edu.sg (S.H. Yeo), ling@ntu.edu.sg (K.V. Ling).

1350-4533/$ – see front matter © 2011 IPEM. Published by Elsevier Ltd. All rights reserved.
doi:10.1016/j.medengphy.2011.09.002

Table 1
Comparison of works that used vibrotactile feedback.

Work	Purpose	Body part measured	Measurement device	Vibrotactile device
[5]	Balance training	Trunk (mediolateral sway)	Microstrain Inertia-Link IMU	Tactaid VBW32 (4 units)
[12]	Motor learning	Arm (5DOF)	Vicon	Tactaid (8 units)
[13]	Risk fall indicator	Trunk (mediolateral sway)	IMU	Tactaid VBW32 (48 units)
[14]	Gesture correction	Upper body (14DOF)	Vicon	SHAKE
[16]	Motion replication	Arm (5DOF)	K-Health IMU	Solarbotics VPM2 (3 units)

to be measured. The key is the protocol that allows optimum conveyance of feedback information to the users while using the minimum number of vibrotactile motors. While other works have used inertia-based sensors and vibrotactile feedback in various applications, ours focuses particularly on rehabilitation, where accurate posture measurement and timely feedback could aid the patient in regaining lost muscular abilities.

The rest of the paper is organized as follows. Section 2 introduces the mathematical foundations of using IMU to measure and correct arm posture. Section 3 discusses the method for guiding arm posture correction while Section 4 presents the system design and method implementation. Section 5 details the experimental setup and Section 6 presents the experimental results. Section 7 concludes the paper and lists future work.

2. Measuring and correcting arm posture

2.1. Working principle of the IMU sensor

Each inertial measurement unit (IMU) sensor has an accelerometer, a magnetic sensor and two gyroscopes inside. The IMU's roll (φ) is the angle measured around the x-axis (parallel to the ground), its pitch (ρ) is the angle around the y-axis (parallel to ground), and its yaw (θ) is the angle around the z-axis (parallel to gravity). The IMU with its orientation axes is shown in Fig. 1(a).

The orientation of the IMU $[\varphi_{acc}(t)\ \rho_{acc}(t)\ \theta_{acc}(t)]$, is derived from the angular velocities $[\omega_x\ \omega_y\ \omega_z]$ about the three axes of the gyroscope. The angular displacements are calculated by integrating the angular velocities:

$$\begin{aligned}\varphi_{gyro} &= \int_{t_i}^{t_f} \omega_x\, dt \\ \rho_{gyro} &= \int_{t_i}^{t_f} \omega_y\, dt \\ \theta_{gyro} &= \int_{t_i}^{t_f} \omega_z\, dt\end{aligned} \tag{1}$$

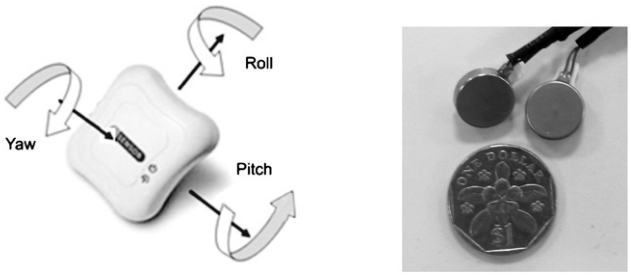

(a) The inertial measurement unit (IMU) sensor, with its axes shown. (b) The vibrotactile actuators.

Fig. 1. The sensors and actuators.

Given the angular value at $(t-1)$ and Δt, the numerical approximation becomes:

$$\begin{aligned}\varphi_{gyro}(t) &= \varphi_{gyro}(t-1) + \omega_x \Delta t \\ \rho_{gyro}(t) &= \rho_{gyro}(t-1) + \omega_y \Delta t \\ \theta_{gyro}(t) &= \theta_{gyro}(t-1) + \omega_z \Delta t\end{aligned} \tag{2}$$

We use the accelerometer measurement to correct for the gyroscope integration error. Finally we obtain the rotation matrix:

$$\mathbf{R} = \begin{bmatrix} r_{11} & r_{12} & r_{13} \\ r_{21} & r_{22} & r_{23} \\ r_{31} & r_{32} & r_{33} \end{bmatrix} \tag{3}$$

where,

$$\begin{aligned} r_{11} &= \cos(\varphi)\cos(\rho) \\ r_{12} &= -\sin(\varphi)\cos(\theta) + \cos(\varphi)\sin(\rho)\sin(\theta) \\ r_{13} &= \sin(\varphi)\sin(\theta) + \cos(\varphi)\sin(\rho)\cos(\theta) \\ r_{21} &= \sin(\varphi)\cos(\rho) \\ r_{22} &= \cos(\varphi)\cos(\theta) + \sin(\varphi)\sin(\rho)\sin(\theta) \\ r_{23} &= -\cos(\varphi)\sin(\theta) + \sin(\varphi)\sin(\rho)\cos(\theta) \\ r_{31} &= -\sin(\rho) \\ r_{32} &= \cos(\rho)\sin(\theta) \\ r_{32} &= \cos(\rho)\cos(\theta). \end{aligned} \tag{4}$$

2.2. Arm model

Fig. 2 illustrates the two arm segments (upper arm and forearm); each has distinct curvature and range of motion. Arm motion, particularly of the elbow and the wrist, can be modeled as a compound flexible pole (CFP). A flexible pole is capable of bending and rotating in three dimensions with no significant deformation along its length.

Each arm segment is modeled as a CFP, a rigid body with an IMU sensor attached, and treated as massless for orientation

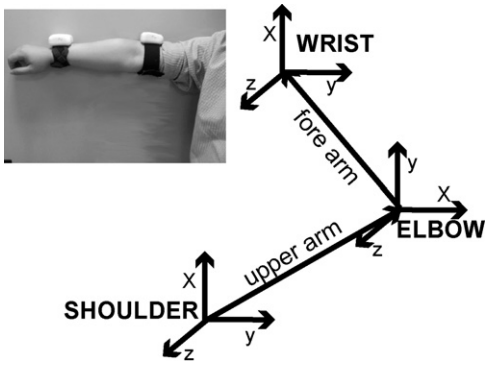

Fig. 2. A compound flexible pole model divides the arm into two main sections: the forearm and the upper-arm. The inset shows where the two IMU sensors are mounted on the arm.

measurements. Modeling the arm as such allowed the expression of the arm motion in the more intuitive form of rotation, flexion–extension and lateral bending. Moreover, this arrangement enables measurement of the whole arm at two strategic points: the shoulder and the wrist.

2.3. Orientation and position measurement

The orientation of the upper arm ($\varphi_u(t)\ \rho_u(t)\ \theta_u(t)$) is derived from the elbow measurements. Using Eq. (2), elbow (x_u, y_u, z_u) and wrist (x_f, y_f, z_f) positions become:

$$\begin{bmatrix} r^u_{11} & r^u_{12} & r^u_{13} & 0 \\ r^u_{21} & r^u_{22} & r^u_{23} & 0 \\ r^u_{31} & r^u_{32} & r^u_{33} & 0 \\ 0 & 0 & 0 & 1 \end{bmatrix} \begin{bmatrix} L_u \\ 0 \\ 0 \\ 1 \end{bmatrix} = \begin{bmatrix} x_u \\ y_u \\ z_u \\ 1 \end{bmatrix} \text{ and} \tag{5}$$

$$\begin{bmatrix} r^f_{11} & r^f_{12} & r^f_{13} & x_u \\ r^f_{21} & r^f_{22} & r^f_{23} & y_u \\ r^f_{31} & r^f_{32} & r^f_{33} & z_u \\ 0 & 0 & 0 & 1 \end{bmatrix} \begin{bmatrix} L_f \\ 0 \\ 0 \\ 1 \end{bmatrix} = \begin{bmatrix} x_f \\ y_f \\ z_f \\ 1 \end{bmatrix}, \tag{6}$$

where L_f is the forearm length and L_u is the upper arm length.

Moreover, given that the upper arm and the forearm form a triangle with vertices at the wrist, elbow, and shoulder:

$$x_f^2 + y_f^2 + z_f^2 = L_u^2 + L_f^2 - 2L_uL_f\ \cos(\gamma_e) \tag{7}$$

The joint angle of elbow γ_e is derived as:

$$\gamma_e(t) = \arccos(-\cos(\theta_f(t) - \theta_u(t))\cos(\rho_f(t))\cos(\rho_u(t)) - \sin(\rho_f(t))\sin(\rho_u(t))) \tag{8}$$

Thus, the elbow angle γ_e is directly related to the upper arm $[\rho_u(t)\ \theta_u(t)]$ and the forearm $[\rho_f(t)\ \theta_f(t)]$ orientations.

2.4. Coordinate calibration with respect to the elbow joint angle

Each IMU sensor is referenced with respect to the shoulder such that the coordinate system of each arm segment and the attached IMU are coupled together; the x-axis lies along the arm length and the z-axis is against gravity vector. To correct for the IMU sensor's displacement offset, users straighten their whole arm, making sure that their elbow reaches 180°. Then, the orientation of the inertia sensors are recorded and the rotation matrices of the displacement offsets are calculated as $R_u^{-1}(0)$ and $R_f^{-1}(0)$. The rectified rotation matrices of the elbow and the wrist become $R_u(t)R_u^{-1}(0)$ and $R_f(t)R_f^{-1}(0)$, respectively.

3. Posture correction protocol

A user's current posture and a reference posture are considered matched if and only if the orientation difference between them is within permissible range. Generally, there are two ways to control posture orientation: orientation trajectory control and position control. Here we propose to use orientation posture matching approach, wherein users adjust their posture in the following order:

1. 3D orientation (yaw, pitch, roll) of the upper arm;
2. Elbow joint angle; and
3. Forearm orientation.

The orientation deviation $\Delta\theta_u$ of the upper arm yaw axis is derived from the orientation of the reference posture – upper arm $[\varphi_{u,r}\ \rho_{u,r}\ \theta_{u,r}]$ and forearm $[\varphi_{f,r}\ \rho_{f,r}\ \theta_{f,r}]$. Then the user moves his arm to reach the posture with $\Delta\theta_u$ within the permissible range of the reference posture. The same method is applied to adjust $\Delta\rho_u$ and $\Delta\varphi_u$.

After correcting the orientation of the upper arm, the elbow angle deviation $\Delta\gamma_e$ is corrected, followed by the forearm roll deviation $\Delta\varphi_f$. To achieve this, the user moves his arm until his elbow reaches the posture with $\Delta\gamma_e$ within the permissible range. Lastly, the user repeats the same process for the forearm roll to attain the posture with $\Delta\varphi_f$ within the acceptable range.

To summarize, users need to adjust the orientation of θ_u, ρ_u, φ_u, γ_e and φ_f, in this particular sequence, when correcting for the reference posture. With this protocol, we were able to use the minimum number of vibrotactile actuators for feedback.

4. System design and implementation

The main components of the system are the inertia sensors (IMU) and the vibrotactile actuators.

4.1. Integrated vibrotactile inertial measurement unit

A wearable vibrotactile inertial measurement unit (VIMU) system integrates three major components: a digital signal controller (DSC), two inertia-based sensors (IMUs), and a vibrotactile-based motion indicator.

4.1.1. Digital signal controller

The DSC, which controls the vibrotactile actuators, is a low-power 8-bit ATMEL ATmega168 Micro Controller Unit (MCU) based on the AVR enhanced RISC architecture. In our prototype the MCU is embedded in an Arduino Duemilanove, an I/O development board. It is both computing platform and development environment for the system's software.

4.1.2. Inertial measurement unit (IMU)

Each IMU provides drift-free orientations and calibrated 3 DOF linear accelerations (from the accelerometer), 3 DOF angular velocities (from the gyroscopes) and 3 DOF magnetic data (from the magnetometer). The accelerometer is a dual-axis low g MEMS-based capacitive ADXL320 from Analog Devices. It is capable of measuring linear acceleration signals over a bandwidth of 60 Hz and has an effective sensing range of ±2 g/±6 g. The magnetometer is a tri-axis magnetic field sensing module HMC1053 from Honey Well. It has a measurement range of ±6 Gauss and capable of measuring the geomagnetic vector. The pair of gyroscopes, dual-axis gyroscopes from Silicon Sensing System (Japan), measures tri-axis angular velocities with a measurement range of ±300 °/s in yaw, and ±500 °/s in roll and pitch.

We developed the software to capture and process the IMU data into rotation, flexion–extension and lateral bending parameters. The data is transferred to a computer via wireless channels, making the whole system portable.

4.1.3. Vibrotactile actuator (tactor)

The feedback unit uses vibrotactile actuators (tactors), small transducers designed to optimize skin response to vibration. The tactors are small flat type (VPM2) and consume little power but provide adequate vibrating strength. They are manufactured by Solarbotics (Calgary, Canada) and shown in Fig. 1(b). Each tactor is activated at the 80–250 Hz frequency range and converts electrical energy into mechanical displacement by using DC power to rotate an eccentric weight. With a 3 V driving voltage each tactor is able to generate 1 g (9.8 m/s^2) acceleration vibration level, which

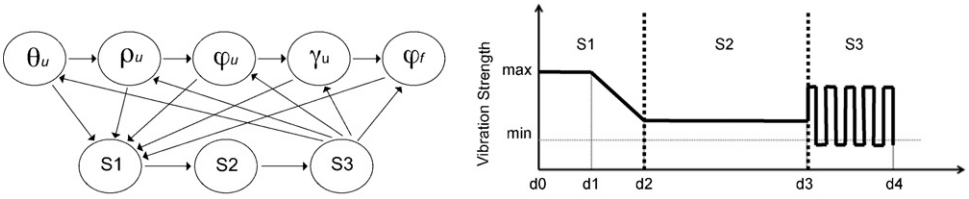

(a) Illustration of the finite state machine that determines the transition for correcting posture orientation parameters.

(b) The vibration pattern associated with each controller state.

Fig. 3. Details of the feedback system design.

is higher than the discrimination thresholds of the forearm and the upper arm, 0.6 g and 0.8 g, respectively [17].

4.2. Placement of tactors on the human body

Based on the study of skin reaction to vibrotactile feedback, two adjacent vibrotactile actuators must have a minimum critical distance in order for their vibration to be distinguishable [18–24]. This threshold varies depending on tactor placement. For forearm placement, the minimum threshold for both men and women is about 40 mm while for the forearm, the threshold is 48 mm for men and 42 mm for women. For optimal perception in the forearm, the threshold can be increased to 50 mm [18].

4.3. Two-tactor feedback to guide motion of a 5 DOF arm

In this section we define the arm posture correction protocol when used with a 2-tactor feedback setup. As of this point, it is assumed that arm posture is obtainable through the IMUs and the thresholds for each posture parameter have already been defined.

Fig. 3(a) shows the complete posture correction process where each posture parameter θ_u, ρ_u, φ_u, γ_e, and φ_f follow the same control scheme. The controller goes through the states S_1, S_2, and S_3 while minimizing the orientation deviation between user and reference postures. The states are defined as follow:

S1 "Correct target direction" indication: At this state, the tactor vibrates at a constant magnitude as the user moves his arm in search for the correct direction. When the limb starts moving to the correct direction, the controller will release a diminishing linear proportional vibration pattern.

S2 "Continue moving to target" indication: The controller will examine in real-time if the orientation deviation falls within a small range, i.e., the user is not radically changing his direction. If deviation is within range, the controller provides a constant vibration pattern to let the user know that he must continue moving in the same direction at constant speed.

S3 "Closing in on the target" indication: Once the orientation deviation is within the threshold value, the controller will produce a burst-like pattern to indicate that the subject is close to the reference. Once the parameter orientation is within the permissible range, the tactor stops vibrating and the controller waits to process the next parameter.

The vibration pattern associated with each state is illustrated in Fig. 3(b).

By correcting the posture in series, our system can afford to use only two tactors for feedback. The feedback toggles between the two tactors to provide the necessary information to the subjects. That is, given two tactors T_a and T_b: during the correction of the first parameter θ_u, T_a will provide the feedback. Then, for the next parameter ρ_u, T_b will provide the feedback. For the third parameter, φ_u, feedback reverts to T_a. For the last two parameters, γ_e and φ_f, feedback is handled by T_b and T_a, respectively.

5. Experimental setup

5.1. Subjects

Five students from the university, with ages ranging from 20 to 27 years, volunteered to participate in the experiments. All were healthy and without any medical condition that could have affected their tactile sensitivity.

5.2. Hardware setup

The two tactors were placed around the subject's arm. The distance between the two tactors was larger than the two-point

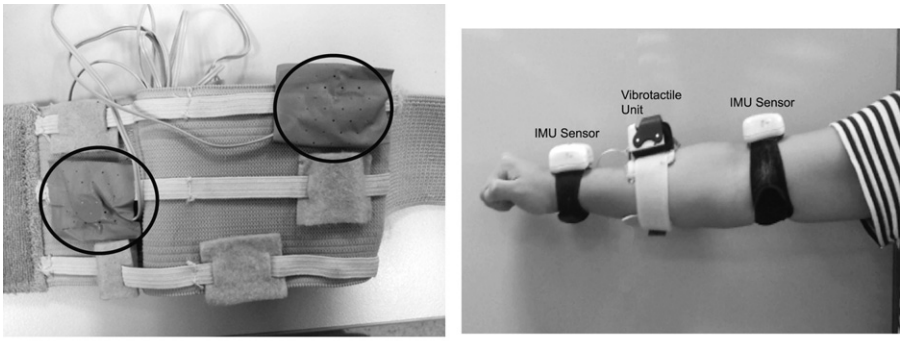

(a) The vibrotactile unit.

(b) Sensors and vibrotactile unit

Fig. 4. The location of the vibrotactile actuators is encircled in (a). The relative position of the sensors and the feedback unit on the arm (b).

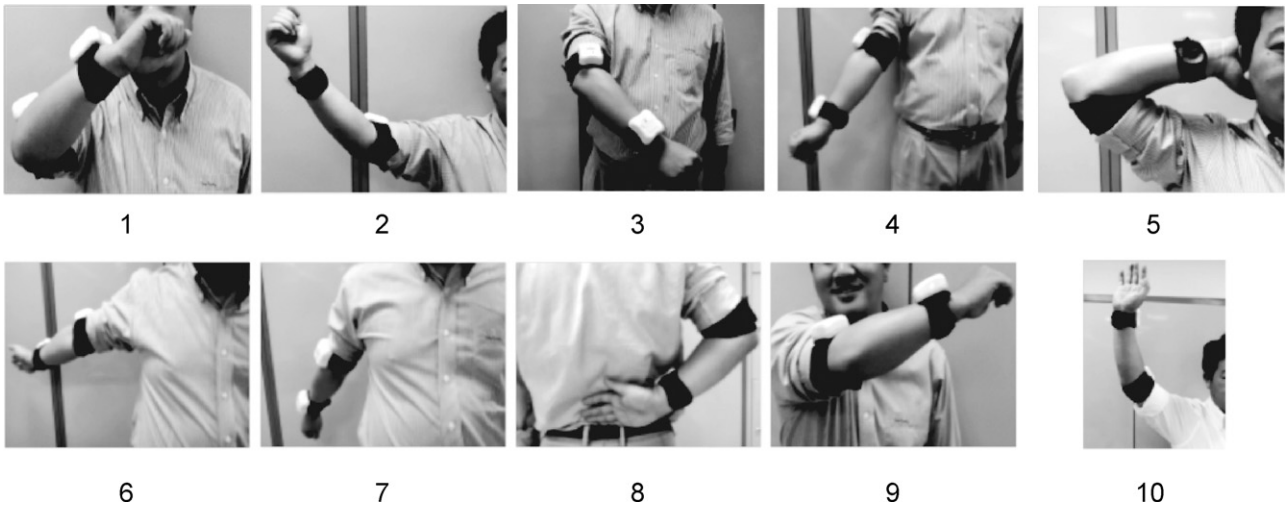

Fig. 5. The ten postures used in the experiments.

discrimination threshold for both male and female [18]. The tactors, secured in a holder, were attached to elastic bands to fit the arm of different subjects. The materials chosen for the tactor holders were thin and soft to ensure vibration detection. The whole vibrotactile unit was light weight, comfortable to use, and easy to wear. Fig. 4(a) shows the inner side of the vibrotactile feedback unit. The digital controller is mounted on the other side of the strap.

5.3. General procedure

The experiment required a master, who establishes the reference posture, and students, who must copy the reference posture. Students were not allowed to see the master's posture; they had to rely solely on the vibrotactile feedback to correct their posture. Prior to each experiment, students practiced several times until they became familiar with interpreting the vibrotactile signal and moving to the indicated direction. The training process required the students to turn their upper arm left and right around the yaw axis, up and down around the pitch axis, and to rotate around the roll axis.

For each experiment, the following procedures were followed:

1. The master wears two IMUs and assumes the target posture.
2. A student wears two IMUs and one vibrotactile unit as shown in Fig. 4(b).
3. The student faces in the same direction as the master and then stretches his whole arm to assume the starting position.
4. The student holds his upper arm for about half a second to check whether tactor A is giving a bursting vibration pattern before correcting for the upper arm's yaw orientation. If the tactor is already vibrating in a burst pattern, then the current upper arm position is already within the correct yaw angle and only needs minor adjustment. Otherwise, the student must start correcting for the pitch orientation.
5. The student must continue moving his arm in the current direction of motion if a decreasing vibration strength is sensed; otherwise the student must move his arm to the opposite direction.
6. The student must slow down to get to the target position when a burst vibration pattern is sensed. When target is reached, the vibration signal will toggle from tactor A to tactor B, indicating the beginning of correction of the next parameter.
7. Steps 4–6 are repeated for the next posture parameter until all parameters are exhausted.

To be able to compare posture among different subjects, the master's postures were recorded. Thus, for all the experiments the

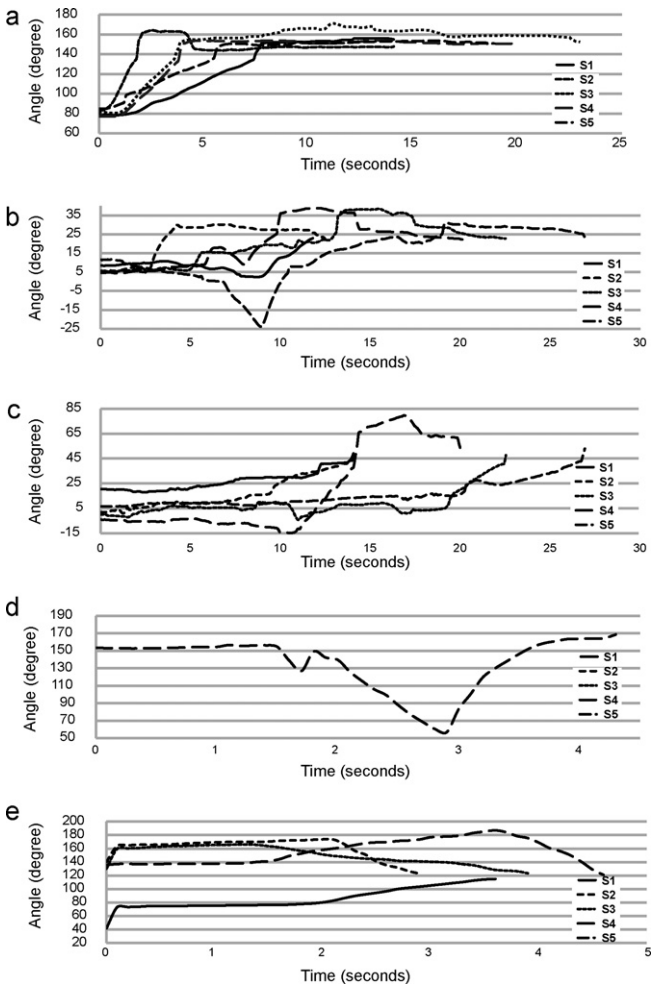

Fig. 6. Results of replicating Posture 1 by five students. (a) Upper arm yaw; (b) upper arm pitch; (c) upper arm roll; (d) elbow joint; (e) forearm roll.

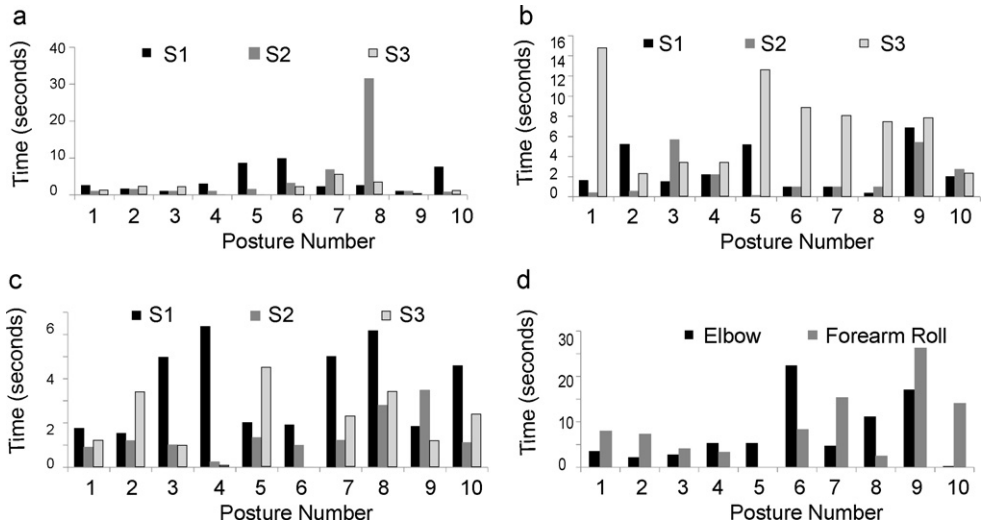

Fig. 7. Average correction time of the ten postures according to individual DOF. (a) Upper arm yaw; (b) upper arm pitch; (c) upper arm roll; (d) elbow angle and forearm roll. **S1**, **S2**, and **S3** refer to the states as illustrated in Fig. 3 (b).

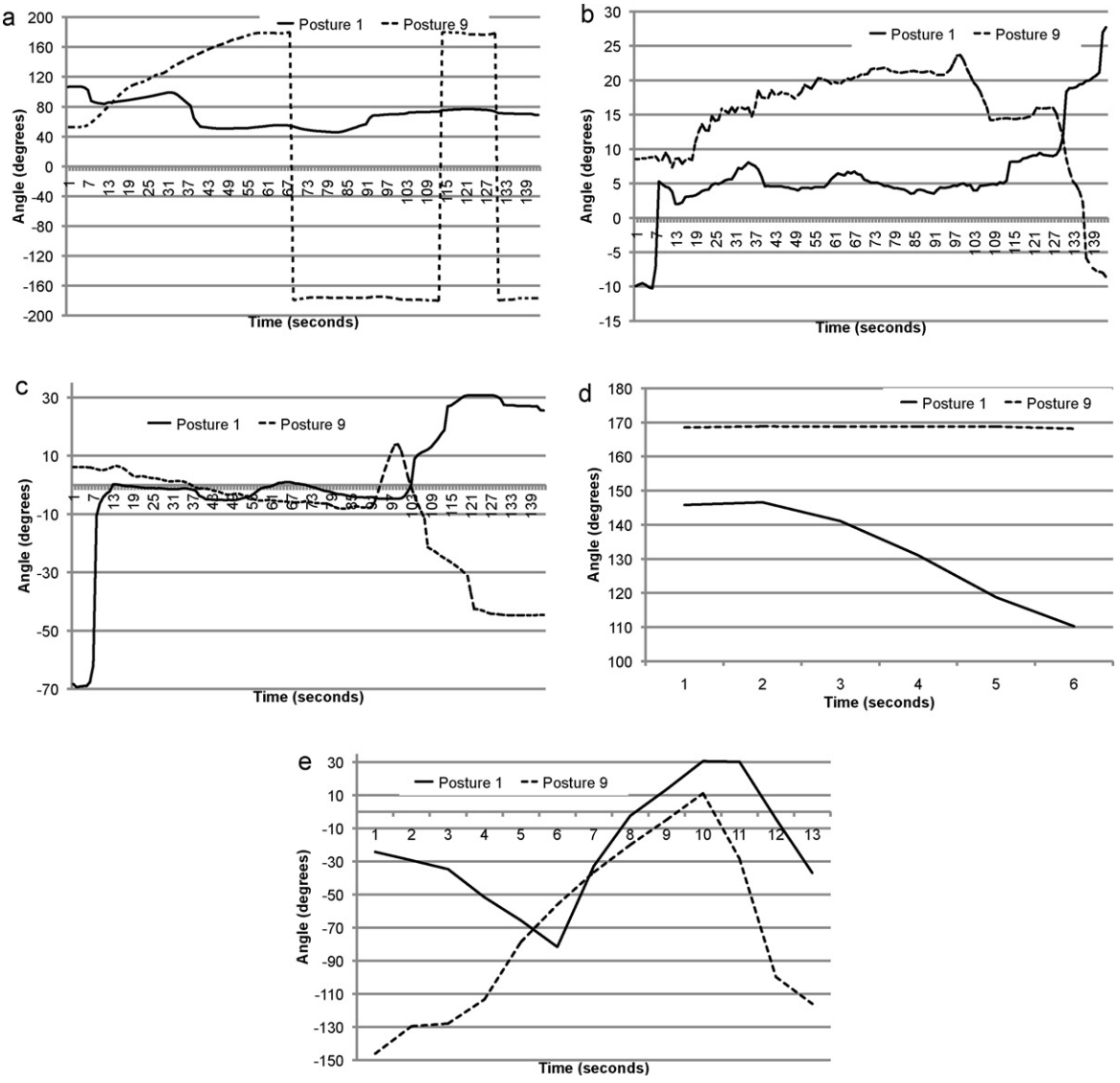

Fig. 8. Trajectory of Postures 1 and 9. (a) Trajectory of the upper arm's yaw; (b) trajectory of the upper arm's pitch; (c) trajectory of the upper arm's roll; (d) trajectory of the elbow angle; (e) trajectory of the forearm's roll.

Table 2
Average user correction time for the ten postures.

Posture	Correction time (s)
1	36.67 ± 6.53
2	28.97 ± 3.62
3	27.54 ± 4.66
4	27.29 ± 5.39
5	41.25 ± 5.02
6	58.61 ± 2.56
7	53.30 ± 2.86
8	72.06 ± 9.40
9	73.32 ± 7.70
10	38.97 ± 7.35

pre-recorded master's postures were just loaded from computer memory.

6. Results and discussion

To check the feasibility of our system ten postures were tested based on arm movement in 3D space, which had been divided into eight zones. The postures are shown in Fig. 5.

The first four zones are at the anterior: left-up, right-up, left-down and right-down (Postures 1, 2, 3, and 4). Similarly, there are four zones at the posterior (Postures 5, 6, 7, and 8). Two additional postures outside of the defined zones were also tested. In Posture 9, part of the forearm passes through the left side of the body. This posture seldom happens in daily activity except when stretching the arm during exercise warm-up. Although Posture 10 is a common one, the forearm is placed higher than the head, which requires additional effort to reach. Thus, each of the ten postures stands for some unique spatial orientation of the arm. In particular, orientations of Postures 6–9 are special because they need more effort to achieve, usually through extra muscle exertion.

Fig. 6 shows the result of replicating Posture 1. The upper arm's yaw, pitch and roll angles for this posture were 148°, 26°, and 53°, respectively. The threshold for successful mapping was set at ±5°. The graphs show that all five subjects were able to move towards the target posture within 30 s. This result indicates that the subjects were able to sense in a timely manner the vibration pattern, which told them when to continue moving in a particular direction and when to stop.

The motion speed, represented by the graph's slopes, varies from subject to subject. Looking at Subject 2 (data labeled **S2**) in Fig. 6(a), the graph shows that he was moving faster compared to the other subjects. However, due to his speed he overshot the target angle and went past the "closing in on" state (state **S3**). Luckily, he felt the quick-burst vibration pattern which quickly made him adjust his movement and went back to state **S3**. After some fine adjustments, he reached the desired yaw angle of 148 ± 5°. His whole posture correction process took 15 s.

Fig. 6(d) and (e) also shows the posture replication for the elbow and the forearm. The elbow and forearm roll reference angles were 171° and 120°, respectively, and the threshold was also set to ±5°. For Subjects 1–5, the initial elbow angles were 170°, 166°, 154°, 170°, and 171°. With the exception of Subject 3, all the other subject's elbow angle were within the threshold (the lines for the other subjects are too short that they are nearly invisible in the graphs). Nevertheless, it took less than 5 s for Subject 3 to correct his elbow angle. The results for mapping the forearm's roll angle were similar, all subjects were able to reach the target posture within 5 s.

Table 2 lists the average time to reach the desired posture for each subject. For postures that appear natural, such as Postures 1, 2, 3, 4, and 10, the subjects reached them within 40 s. However, the subjects had to spend more time on Postures 6, 7, 8, and 9, with mapping time ranging from 50 to 70 s.

Fig. 7 shows the average correction time of all users for each arm posture parameter. The correction time for the upper arm (Fig. 7(a–c)) was further divided into different phases that correspond to the vibration feedback control states. Upper arm yaw mapping required more time during the **S2** phase, while the upper arm pitch mapping required more time during the **S3** phase. Compared to correction of the elbow joint angle, correction of the forearm's roll took longer (Fig. 7(d)).

In Fig. 8, the trajectory of Posture 1 is smoother than that of Posture 9. The subject took more time in correcting the forearm's roll angle as shown in Posture 9. However, it is reasonable to assume that in order to complete Posture 9, the subject had to stretch his arm longer and farther.

7. Conclusion

In this paper, we presented a guidance system that helps subjects replicate a reference arm posture using inertia-based sensors and vibrotactile feedback. Our system supports real-time arm posture measurement and orientation feedback generation. We tested our system with several subjects using ten postures that represent different arm configurations in 3D space. All the subjects managed to reach the target posture, with varying performance, usually depending on the difficulty of the posture.

Our future work includes several tasks. First, the protocol for posture correction needs modification if dynamic body movements will be used. As some postures can be difficult to replicate, additional feedback mode might be necessary to maintain fast posture correction. Testing of our system in actual rehabilitation setting with stroke patients is currently under consideration.

The posture correction system that we have developed is small, wearable, and non-intrusive, making it ideal for therapy sessions and for extended wear. Patients can use the system to undergo rehabilitation with minimal therapist supervision (such as in remote rehabilitation), freeing therapist's time while empowering the patients to take control of their own therapy.

Acknowledgements

This work was supported in part by the Agency for Science, Technology and Research, Singapore, under SERC Grant 092 149 0082, and Media Development Authority, Singapore under NRF IDM004-005 Grants.

The authors would like to thank Wei-Ting Yang, Ni Wei, Guo Wen Jiang and Yuan Qi Long for their continuous advice and assistance on the design of the vibrotactile feedback and inertial measurement unit.

Conflict of interest

We also certify that no actual or potential conflict of interest in relation to this article exists.

References

[1] Rosati G. The place of robotics in post-stroke rehabilitation. Expert Rev Med Devices Nov 2010;7(6):753–8.
[2] Beer RF, Dewald JPA, Dawson ML, Rymer WZ. Target-dependent differences between free and constrained arm movements in chronic hemiparesis. Exp Brain Res 2004;156(4):458–70.
[3] Bazzarelli M, Durdle NG, Lou E, Raso VJ. A wearable computer for physiotherapeutic scoliosis treatment. IEEE Trans Instrum Meas 2003;51(February (1)):126.
[4] Keijsers NLW, Horstink MWIM, Gielen SCAM. Online monitoring of dyskinesia in patients with Parkinson's disease. IEEE Eng Med Biol 2003;22(3):96.
[5] Alahakone AU, Arosha Senanayake SMN. A real-time system with assistive feedback for postural control in rehabilitation. IEEE-ASME Trans Mech 2010;15(April (2)):226–33.

[6] Zhu R, Zhou Z. A real-time articulated human motion tracking using tri-axis inertia/magnetic sensors package. IEEE Trans Neural Syst Rehabil Eng 2004;12(June (2)):295–302.
[7] Moe-Nilssen R, Helbostad JL. Estimation of gait cycle characteristics by trunk accelerometry. J Biomech 2004;37(January (1)):121–6.
[8] Matjacic Z, Hunt K, Gollee H, Sinkjaer T. Control of posture with FES systems. Med Eng Phys 2003;25(January (1)):51–62.
[9] O'Dwyer SB, O'Keeffe DT, Coote S, Lyons GM. An electrode configuration technique using an electrode matrix arrangement for FES-based upper arm rehabilitation systems. Med Eng Phys 2006;28(March (2)): 166–76.
[10] Van Viet P, Wulf G. Extrinsic feedback for motor learning after stroke: what is the evidence? Disabil Rehabil 2006;28(13–14):831–40.
[11] Giansanti D, Dozza M, Chiari L, Maccioni G, Cappello A. Energetic assessment of trunk postural modifications induced by a wearable audio-biofeedback system. Med Eng Phys 2009;31(January (1)):48–54.
[12] Lieberman J, Breazeal C. TIKL: development of a wearable vibrotactile feedback suit for improved human motor learning. IEEE Trans Robot 2007, October;23:919–26.
[13] Wall III C, Wrisley DM, Statler KD. Vibrotactile tilt feedback improves dynamic gait index: a fall risk indicator in older adults. Gait Posture 2009;30(July (1)):16–21.
[14] Portillo-Rodriguez O, Sandoval-Gonzalez O, Ruffaldi E, Leonardi R, Avizzano C, Bergamasco M. Real-time gesture recognition, evaluation and feed-forward correction of a multimodal Tai-Chi platform. In: Lect notes comput sc: haptic and audio interaction design, vol. 5270. 2008. p. 30–9.
[15] Luo ZQ, Lim CK, Yang WT, Tee KY, Li K, Gu C, et al. An interactive therapy system for arm and hand rehabilitation. In: Proc. of the IEEE conf. on robotics automation and mechatronics, Singapore. 2010. p. 9–14.
[16] Ding ZQ, Chen IM, Yeo SH. Development of a real-time wearable motion replication platform with spatial sensing and tactile feedback. In: Proc. IEEE/RSJ int. conf. on intelligent robots and systems. 2010, October.
[17] Lynette AJ, David AH. A characterization of tactors used in vibrotatile displays. J Comput Inf Sci Eng 2008, December;8, 044501-1–044501-5.
[18] Myles K, Binseel MS. The tactile modality: a review of tactile sensitivity and human tactile interfaces, U.S. Army Research Laboratory, ARL-TR-4115, Aberdeen Proving Ground, MD 21005-5425; 2007, May.
[19] Johansson RS. Tactile sensibility in the human hand: receptive field characteristics of mechanoreceptive units in the glabrous skin. J Physiol 1978;281:101–23.
[20] Bolanowski SJ, Gesheider GA, Verrillo RT, Checkosky CM. Four channels mediate the mechanical aspects of touch. J Acoust Soc Am 1988;84(5):1680–94.
[21] Kuc R. Bianaural sonar electronic travel aid proves vibrotactile cues for landmark, reflector motion and surface texture classification. IEEE Trans Biomed Eng 2002;49:1173–80.
[22] Moore TJ, Mundie RJ. Measurement of specific mechanical impedance of the skin: effects of static force, site of stimulation, area of probe and presence of a surround. J Acoust Soc Am 1972;52:577–84.
[23] Eskildsen P, Morris A, Collins CC, Bach-Y-Rita P. Simultaneous and successive cutaneous two-point threshold for vibration. Psychon Sci 1969;14:146–7.
[24] Mizuno T, Uchida M, Ide H. A basic study on tactile navigation using vibration motor braking by skin against vibration and body positioning suitable for tactile information presentation. J Robot Mechatron 2008, April;20:501–6.